HIV-1 Vpu Blocks Recycling and Biosynthetic Transport of the Intrinsic Immunity Factor CD317/Tetherin To Overcome the Virion Release Restriction

Sarah Schmidt, Joëlle V. Fritz, Julia Bitzegeio,* Oliver T. Fackler, and Oliver T. Keppler

Department of Infectious Diseases, Virology, University of Heidelberg, Heidelberg, Germany

* Present address: Aaron Diamond AIDS Research Center, New York, New York, USA.

S.S. and J.V.F. contributed equally to this work.

ABSTRACT **The intrinsic immunity factor CD317 (BST-2/HM1.24/tetherin) imposes a barrier to HIV-1 release at the cell surface that can be overcome by the viral protein Vpu. Expression of Vpu results in a reduction of CD317 surface levels; however, the mechanism of this Vpu activity and its contribution to the virological antagonism are incompletely understood. Here, we characterized the influence of Vpu on major CD317 trafficking pathways using quantitative antibody-based endocytosis and recycling assays as well as a microinjection/microscopy-based kinetic *de novo* expression approach. We report that HIV-1 Vpu inhibited both the anterograde transport of newly synthesized CD317 and the recycling of CD317 to the cell surface, while the kinetics of CD317 endocytosis remained unaffected. Vpu trapped trafficking CD317 molecules at the *trans*-Golgi network, where the two molecules colocalized. The subversion of both CD317 transport pathways was dependent on the highly conserved diserine S52/S56 motif of Vpu; however, it did not require recruitment of the diserine motif interactor and substrate adaptor of the SCF-E3 ubiquitin ligase complex, β-TrCP. Treatment of cells with the malaria drug primaquine resulted in a CD317 trafficking defect that mirrored that induced by Vpu. Importantly, primaquine could functionally replace Vpu as a CD317 antagonist and rescue HIV-1 particle release.**

IMPORTANCE **HIV efficiently replicates in the human host and induces the life-threatening immunodeficiency AIDS. Mammalian genomes encode proteins such as CD317 that can inhibit viral replication at the cellular level. As a countermeasure, HIV has evolved genes like *vpu* that can antagonize these intrinsic immunity factors. Investigating the mechanism by which Vpu overcomes the virion release restriction imposed by CD317, we find that Vpu subverts recycling and anterograde trafficking pathways of CD317, resulting in surface levels of the restriction factor insufficient to block HIV-1 spread. This describes a novel mechanism of immune evasion by HIV.**

Received 28 February 2011 **Accepted** 25 April 2011 **Published** 24 May 2011

Citation Schmidt S, Fritz JV, Bitzegeio J, Fackler OT, Keppler OT. 2011. HIV-1 Vpu blocks recycling and biosynthetic transport of the intrinsic immunity factor CD317/tetherin to overcome the virion release restriction. mBio 2(3):e00036-11. doi:10.1128/mBio.00036-11.

Invited Editor Akira Ono, University of Michigan Medical School **Editor** Vinayaka Prasad, Albert Einstein College of Medicine

Address correspondence to Oliver T. Fackler, oliver.fackler@med.uni-heidelberg.de, or Oliver T. Keppler, oliver.keppler@med.uni-heidelberg.de.

As obligate intracellular parasites, viruses rely for their replication on a wide array of host cell machineries. This intimate relationship is also exploited by the host, which has developed, in addition to adaptive immune responses, innate and intrinsic immune mechanisms to fend off viral intruders. In the case of HIV, the proteins TRIM5α and CD317 (BST-2/HM1.24/tetherin), as well as members of the APOBEC family of cytidine deaminases, are prominent examples of host cell factors that can restrict HIV-1 replication at distinct steps of the viral life cycle. General mechanisms of virus-host coevolution and the high genetic plasticity of the HIV-1 genome have led to the emergence of virus variants that are insensitive to such restrictions. For example, the capsid protein of HIV-1 cannot be efficiently recognized by the human ortholog of TRIM5α (1). As an additional strategy, HIV-1 has evolved accessory genes that are not essential for virus replication *per se*, the expression of which, however, allows the virus to overcome specific restriction factors. The Vif and Vpu proteins, viral antagonists that counteract human APOBEC and CD317 proteins, respectively, thus constitute important genetic adaptations of HIV-1 that facilitate virus replication in the face of an active intrinsic immunity (2).

CD317 is a glycosylated type II transmembrane protein with an unusual topology: it has a short cytoplasmic N terminus, a single membrane-spanning domain, and a large extracellular domain that contains a coiled-coil and that is tethered to cholesterol-rich membrane microdomains by virtue of its glycophosphatidylinositol anchor at the C terminus (3–6). Cell surface CD317 is endocytosed by an AP-2- and clathrin-dependent pathway (7, 8). The fate of internalized CD317 molecules has not been studied in detail; however, it is likely to include a yet-to-be-defined recycling pathway.

In the context of viral infection, CD317 was identified as a potent, type I interferon-induced restriction factor of HIV-1 par-

ticle release that traps mature virions at the surface of virus-producing cells (hence the name "tetherin") (9). This activity requires multimerization of CD317, and the current model suggests that dimers of the restriction factor physically bridge the cell's plasma membrane and nascent virions or bridge virions among each other (5, 9, 10). In addition to preventing the release of virions into the extracellular space, CD317 may also affect the dissemination of HIV-1 particles by the cell-to-cell route (11, 12), although this is still a matter of controversy (13). The antiviral spectrum of CD317 is not restricted to HIV and includes nonhuman primate lentiviruses, simple retroviruses, filoviruses, arenaviruses, rhabdoviruses, influenza virus, and herpesviruses (9, 14–20).

Many of these unrelated viruses encode viral antagonists to overcome the particle release barrier imposed by CD317. In the case of HIV-1, this function is exerted by the accessory protein Vpu. Vpu is a ~16-kDa transmembrane protein that is best studied for its ability to degrade the HIV-1 entry receptor CD4 early during biosynthetic transport (21, 22). Via the substrate recognition unit beta-transducin repeat-containing protein (β-TrCP), Vpu recruits the multisubunit SCF (Skp1/cullin/F-box protein)-E3 ubiquitin ligase complex to the endoplasmic reticulum (ER) and bridges it to newly synthesized CD4 molecules (23). As a consequence, CD4 molecules are retained in the ER followed by targeting to the ER-associated degradation (ERAD) pathway (22, 24). The Vpu–β-TrCP interaction requires a canonical diserine DSGxxS (S52/S56) motif in the cytoplasmic tail of Vpu (23, 25).

The mechanism by which Vpu counteracts CD317 is far less well understood. The diserine motif of Vpu is also involved in antagonism of CD317 (26, 27), and cellular levels of CD317 were frequently found to be decreased in the presence of Vpu (26–29). This led to the hypothesis that, in analogy to its action on CD4, Vpu may counteract CD317 by triggering its degradation. However, the extent of depletion of CD317 cellular pools does not strictly correlate with CD317's ability to rescue HIV-1 particle release (30–32), and a CD317 mutant that is resistant to Vpu-mediated depletion can still be efficiently antagonized (33). Furthermore, the cell surface density of the restriction factor was found to be reduced in the presence of Vpu and in part uncoupled from alterations of levels of intracellular CD317 pools (26, 30, 33, 34). Conceivably, the reduction of CD317's surface levels and thus of the levels at sites of virus budding may be sufficient to account for Vpu's antagonistic virological properties, and so far an inverse relationship between Vpu's effects on CD317 surface exposure and virus production has been noted (26, 30, 33–35). Direct experimental evidence for a cardinal role of CD317 downregulation in Vpu's antagonistic property is, however, lacking. Moreover, by which mechanism Vpu deregulates the CD317 surface density is unclear. Even though a physical interaction between Vpu and CD317 and a colocalization of the two proteins at intracellular membranes within or near the *trans*-Golgi network (TGN) has been reported (30, 36, 37), the specific transport pathway(s) of CD317 affected by Vpu is undefined. A slightly enhanced internalization rate of CD317 (38, 39) or a decreased outward transport of CD317 (30, 37) has recently been suggested, with considerable controversy remaining (40, 41). In the present study, we therefore sought to define the mechanism by which Vpu alters trafficking of CD317 to induce a reduction of the cell surface density of the restriction factor and to analyze whether these alterations in intracellular CD317 transport are critical for Vpu's role as an antagonist of the CD317-imposed HIV-1 release restriction.

RESULTS

HIV-1 Vpu does not affect the internalization rate of CD317. A selective downregulation of cell surface CD317 can be accomplished by three possible mechanisms: (i) an enhanced rate of endocytosis of cell surface CD317 molecules, (ii) a reduced rate of recycling of previously internalized CD317 molecules back to the cell surface, or (iii) a diminished rate of resupply of newly synthesized CD317 from within the cell. We therefore set out to conduct a comprehensive characterization of Vpu's effect on CD317 trafficking in HeLa-derived TZM-bl cells, which express high levels of endogenous CD317 (42).

Internalization of CD317 from the cell surface occurs by a clathrin-dependent pathway (7, 8). Conflicting studies reported either an enhancing effect (38, 39) or no effect (30, 31, 43) of Vpu on CD317 internalization. In the present study, TZM-bl cells were transfected with expression plasmids encoding Vpu.GFP or GFP (green fluorescent protein) alone and analyzed 1 day later by flow cytometry. At steady state, expression of Vpu.GFP reduced surface levels of CD317 to ~35% of those observed in GFP-expressing control cells (see Fig. S1B in the supplemental material). These transfected cells were used in a kinetic antibody (Ab)-based endocytosis assay to determine CD317 internalization kinetics (see schematic in Fig. S1A). First, cells were incubated at 4°C with saturating concentrations of the unconjugated anti-HM1.24/CD317 monoclonal antibody (MAb) that recognizes an epitope in the extracellular domain of CD317 (44). Subsequently, cells were shifted to 37°C for various time periods ($t = 0$ to 40 min), allowing endocytosis of CD317 to occur. Finally, cells were stained with a fluorescently labeled secondary antibody at 4°C to detect the remaining antibody-CD317 complexes at the cell surface by flow cytometry. Employing this protocol, CD317 was internalized at a rate of ~2% per min in GFP-expressing control cells during the first 20 min with a loss of ~50% of the surface pool of CD317 by 40 min (Fig. S1C, filled circles), consistent with dynamics reported in recent studies (30, 31, 43). Importantly, expression of Vpu.GFP significantly affected neither the rate nor the kinetics of CD317 internalization (Fig. S1C, open circles). Comparable results were obtained in TZM-bl cells expressing untagged Vpu together with GFP or when an alternative anti-CD317 antibody (polyclonal rabbit BST-2 antiserum [32]) was used (data not shown). Thus, in agreement with several recent reports (30, 31, 43), Vpu does not significantly alter the endocytosis rate or kinetics of endogenous CD317 in TZM-bl cells.

Establishment and validation of a CD317 recycling assay. To determine if Vpu affects the trafficking of endocytosed CD317 molecules back to the cell surface, we developed an antibody-based recycling assay (see schematic in Fig. 1A). This assay, in contrast to previously reported approaches (45–48), does not rely on harsh protease treatment, acid stripping, radioactive or biotin labeling, or ligand-induced endocytosis. Instead, it kinetically detects CD317 molecules surfacing at the plasma membrane in transfected or infected cells from intracellular pools, into which they had recently been endocytosed. In detail, TZM-bl cells were first incubated at 4°C with saturating concentrations of the unconjugated anti-HM1.24/CD317 MAb. Subsequently, a temperature shift to 37°C for various time periods ($t = 0$ to 12 min) allowed, besides endocytosis of antibody-CD317 complexes, recy-

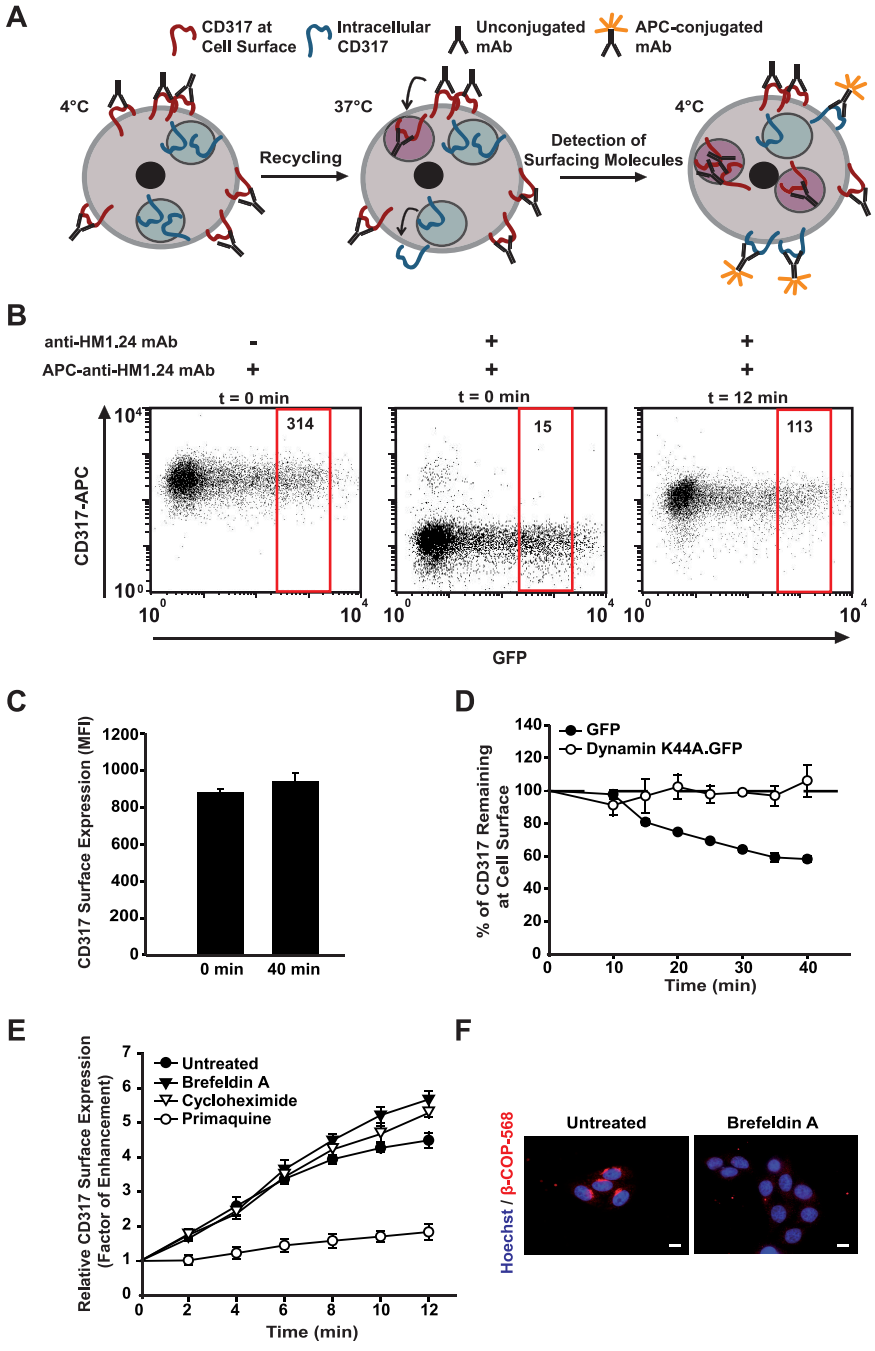

FIG 1 CD317 recycling is rapid and sensitive to primaquine. (A) Schematic representation of an antibody-based recycling assay. For assay validation, TZM-bl cells were transfected with a GFP-expressing plasmid. Twenty-four hours posttransfection, cells' CD317 surface pool was first labeled with saturating concentrations of unconjugated anti-HM1.24/CD317 MAb at 4°C before incubation at 37°C for the indicated time intervals (t = 0 to 12 min) to allow recycling of previously intracellular, unlabeled CD317 molecules (blue). Subsequently, cells were stained with the identical anti-HM1.24/CD317 MAb, covalently conjugated to APC, at 4°C, and the MFI of GFP-positive cells was quantified by flow cytometry. Vesicles with recently internalized cargo are shown in magenta; recycling vesicles are shown in gray. (B) Representative FACS dot plots of CD317-APC staining of transfected TZM-bl cells in the recycling assay at steady state (left), at t = 0 min (middle), and at t = 12 min (right). The red gate depicts the high-GFP-expressing cells, and the respective MFI values are indicated within the gate. (C and D) Anti-HM1.24/CD317 MAb is not shed from antibody-CD317 complexes. (C) TZM-bl cells were first stained with unconjugated anti-HM1.24/CD317 MAb at 4°C, washed, and incubated for either 0 min or 40 min on ice. Antibody-CD317 complexes at the cell surface were subsequently detected with an APC-conjugated secondary antibody at 4°C and quantified by flow cytometry. (D) TZM-bl cells were transfected with expression plasmids encoding either GFP (filled circles) or the dominant negative dynamin K44A.GFP mutant (open circles). Twenty-four hours posttransfection, cells were analyzed in the endocytosis assay as described for Fig. S1A and C. The graph depicts the kinetics of relative CD317 levels remaining at the surface of viable, GFP-positive, or dynamin K44A.GFP-positive cells as relative percentages of the respective MFIs at t = 0 min, which were set to 100%. Shown are the arithmetic means ± standard deviations of triplicates from one experiment. Two independent assays were performed. (E) Recycling assay validation. pGFP-transfected TZM-bl cells were pretreated with either brefeldin A (0.2 mM, 2 h), cycloheximide (0.2 mM, 2 h), or primaquine (0.5 mM, 45 min) or were left untreated and subsequently analyzed in the CD317 recycling assay. The graph depicts the relative cell surface expression of CD317 detected by the APC-conjugated anti-HM1.24/CD317 MAb and is presented as the factor of enhancement of the MFIs at different time points relative to the MFI at t = 0, which was set to 1. Shown are the arithmetic means ± standard deviations of triplicates of one out of three independent experiments. (F) Microphotographs of brefeldin A-treated (0.2 mM, 2 h) and untreated control cells stained for the Golgi apparatus marker β-COP (red). Nuclei were counterstained with Hoechst stain. Scale bars, 10 μm.

cling of intracellular and thus unlabeled CD317 molecules back to the cell surface (Fig. 1A, blue CD317 molecules). These newly surface-exposed molecules were then directly detected using the identical anti-HM1.24/CD317 MAb, which had been covalently coupled to the allophycocyanin (APC) fluorophore. It is important to realize that molecules remaining at the cell surface that still carry the unlabeled MAb cannot be recognized by the identical MAb coupled to APC.

As depicted in the fluorescence-activated cell sorting (FACS) dot plots in Fig. 1B, saturation of pGFP-transfected cells' CD317 surface population with the unconjugated anti-HM1.24/CD317 MAb was efficient, demonstrated by the low background staining with the APC-conjugated MAb (Fig. 1B, middle panel; t = 0 min; mean fluorescence intensity [MFI], 15) compared to that of untreated cells at steady state (Fig. 1B, left panel; MFI, 314). Within 12 min of incubation at 37°C, a prominent population of previously unlabeled CD317 molecules appeared at the cell surface that could be detected by the APC-conjugated anti-HM1.24/CD317 MAb (Fig. 1B, right panel; t = 12 min; MFI, 113).

To evaluate whether shedding of the unconjugated, surface-bound anti-HM1.24/CD317 MAb contributes to the increasing binding of the APC-conjugated antibody in this recycling assay,

two control assays were performed. First, incubation of antibody-labeled cells for 40 min at 4°C, at which temperature receptor endocytosis does not occur, did not result in a reduction of antibody levels, assessed with an APC-conjugated secondary antibody (Fig. 1C). Second, blocking CD317 endocytosis by expression of the dominant negative dynamin K44A.GFP mutant (49) resulted in stable levels of the unconjugated surface-bound anti-HM1.24/CD317 MAb for prolonged periods even at 37°C (Fig. 1D, open circles). Together, these findings demonstrate that significant antibody shedding does not occur and is therefore not a confounding issue in this recycling assay.

Employing this assay, the appearance of previously intracellular CD317 at the surface of untreated TZM-bl control cells was detected at a rate of ~3% per min, resulting in a more than 4-fold increase of CD317 surface levels within 12 min (Fig. 1E, black circles). To discriminate between newly surface-exposed CD317 glycoproteins that originated either from recycling compartments or from the biosynthetic pathway, we inhibited the anterograde transport through the Golgi apparatus by pretreatment of cells with brefeldin A. Despite efficient disruption of the Golgi apparatus (see dispersed β-COP staining in the presence of brefeldin A, Fig. 1F), the rate of CD317 molecules surfacing at the plasma membrane was not diminished (Fig. 1E, black triangles). Similarly, shutdown of *de novo* protein biosynthesis by cycloheximide pretreatment of cells did not affect results of the recycling assay (Fig. 1E, open triangles). CD317 proteins in the anterograde biosynthetic pathway, therefore, do not significantly contribute to the surfacing of CD317 molecules within the 12-min observation period. In sharp contrast, virtually no additional CD317 molecules surfaced in cells treated with primaquine (PQ), a lysosomotropic amine that has a strong inhibitory effect on the recycling of certain receptors (50–52), including major histocompatibility complex (MHC) class II glycoproteins and the transferrin receptor. We conclude that our antibody-based assay specifically and quantitatively detects recycling of previously endocytosed CD317 molecules from intracellular compartments back to the cell surface. We find that CD317 exhibits a fast recycling kinetic that is sensitive to treatment with PQ.

Vpu diminishes CD317 recycling. Next we employed this assay to determine whether HIV-1 Vpu affects the kinetic of CD317 recycling. Parallel analysis of CD4, the major binding receptor of HIV-1, was included as an informative reference since this receptor is targeted by Vpu exclusively in the biosynthetic pathway (21, 22). Transient expression of Vpu.GFP reduced surface levels of both CD317 and CD4 on TZM-bl cells at steady state to similar degrees, by 64 and 54%, respectively, compared to GFP-expressing control cells (Fig. 2A). Cells which expressed Vpu.GFP showed a markedly reduced kinetic of CD317 recycling compared to that of GFP-only controls ($P = 0.018$, Fig. 2B; see also Fig. S2 for data from an independent experiment including primary FACS plots). At 12 min, recycled molecules amounted to an increase of only 3.1-fold (Vpu.GFP) compared to 6.2-fold (GFP) relative to levels at $t = 0$ min (Fig. 2B). Comparable results were obtained upon expression of untagged Vpu together with GFP (Fig. 2C). In contrast, the recycling of CD4 was not inhibited, but rather modestly accelerated, by Vpu.GFP (Fig. 2D), although the reductions of steady-state surface levels of the two receptors were comparable (Fig. 2A). These results underscored the specificity of the assay for the detection of receptors that are recycling from intracellular compartments, and not those in the biosynthetic anterograde

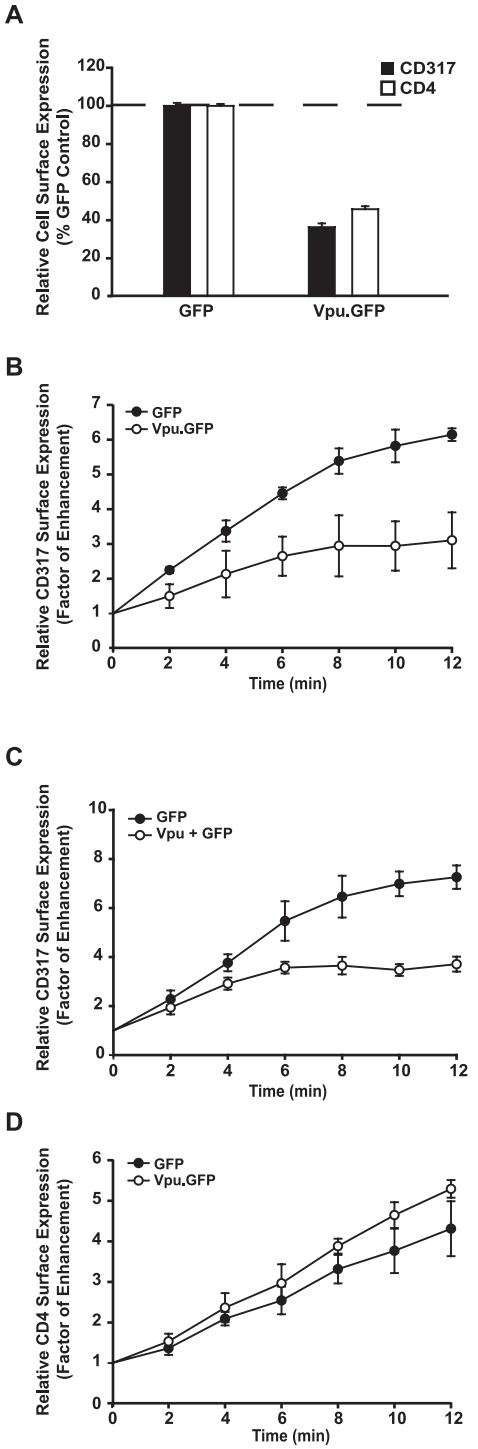

FIG 2 HIV-1 Vpu interferes with the recycling of CD317, but not of CD4. TZM-bl cells were transfected with expression plasmids encoding Vpu.GFP or GFP or cotransfected with expression plasmids for untagged Vpu and GFP (Vpu + GFP). Twenty-four hours posttransfection, cells were stained for surface steady-state levels of either CD317 or CD4 and analyzed by flow cytometry (A), used in a CD317 recycling assay as described in the legend to Fig. 1 (B and C), or used in a recycling assay for CD4, which was performed analogously to that for CD317 (D). Shown are arithmetic means ± standard deviations of triplicates. Seven similar assays were performed for panel B, two similar assays were performed for panel C, and four similar assays were performed for panel D.

transport pathway. Importantly, we pinpoint recycling of CD317 as a trafficking step inhibited by HIV-1 Vpu.

To confirm the impact of Vpu on CD317 recycling in an infection context, TZM-bl cells were challenged with vesicular stomatitis virus G protein (VSV-G)-pseudotyped GFP reporter viruses based on the NL4-3 strain of HIV-1 (53). An internal ribosome entry site (IRES) inserted downstream of the *nef* gene preserves expression of all viral genes and supports long terminal repeat (LTR)-driven GFP expression in infected cells. TZM-bl cells infected with the Vpu-deficient HIV-1 IRES.GFP virus (HIV-1 Δ*vpu* IRES.GFP, Fig. 3A, black circles) displayed CD317 recycling rates that were comparable to those seen in GFP-expressing control cells (compare with Fig. 2B and C). In contrast, recycling of CD317 was impaired in cells infected with the HIV-1 wild-type (wt) IRES.GFP virus compared to those infected with the HIV-1 Δ*vpu* IRES.GFP virus ($P = 0.023$, Fig. 3A, open circles). While being statistically significant, the impact of Vpu expressed from this reporter virus on CD317 recycling in infected TZM-bl cells was slightly less pronounced than that seen for ectopic expression of Vpu or Vpu.GFP. These HIV-1-infected TZM-bl cultures displayed the expected Vpu-dependent virological phenotypes: the wt virus was released more efficiently than its Vpu-negative counterpart (Fig. 3C and 3D) and mediated a reduction of steady-state surface levels of CD317 (Fig. 3B). Furthermore, recycling of endogenous CD317 was also found to be severely impaired in a Vpu-dependent manner in HIV-1-infected Jurkat T cells (Fig. S3). Together, these results demonstrate that Vpu exerts a profound and target molecule-specific inhibitory effect on the recycling of CD317.

Vpu blocks anterograde transport of CD317 to the cell surface. We next asked whether Vpu, in addition to its inhibitory effect on CD317 recycling, can also affect the transport of newly synthesized CD317 molecules to the cell surface. Since the specific analysis of biosynthetic transport is technically challenging, we employed a microscopy-based kinetic *de novo* expression analysis: plasmids encoding CD317, which carries an HA tag embedded in the extracellular domain (CD317-HA_{int}) (35), and pVpu.GFP (or pGFP) were comicroinjected into the nuclei of TZM-bl cells and the localization of newly expressed proteins was analyzed in cells fixed at different time points postinjection.

Protein expression was readily detectable 1 h postinjection by confocal microscopy. At this early time point, CD317-HA_{int} molecules showed a primarily perinuclear, ER-like distribution in GFP-coexpressing control cells, while CD317-HA_{int} localization at the plasma membrane was still rarely observed (Fig. 4A; quantification is shown in Fig. 4E). Already at 2 h, newly synthesized CD317-HA_{int} molecules were detectable at the surface of ~50% of cells, indicative of a rapid transport to the plasma membrane. By 16 h, a strong surface localization was apparent in over 90% of cells in addition to cytoplasmic pools of the restriction factor (Fig. 4C and 4E).

Coexpression of Vpu.GFP, however, had a pronounced effect on the subcellular distribution of newly synthesized CD317-HA_{int}: already at 1 h postinjection CD317 localized to a compact perinuclear compartment (Fig. 4B) morphologically distinct from that observed in the GFP-expressing control cells (Fig. 4A) and consistent with a TGN-like pattern (Fig. 4J) already at this early time point. This predominant perinuclear localization of newly synthesized CD317-HA_{int} frequently persisted in a somewhat more dispersed pattern even at the latest time point (16 h,

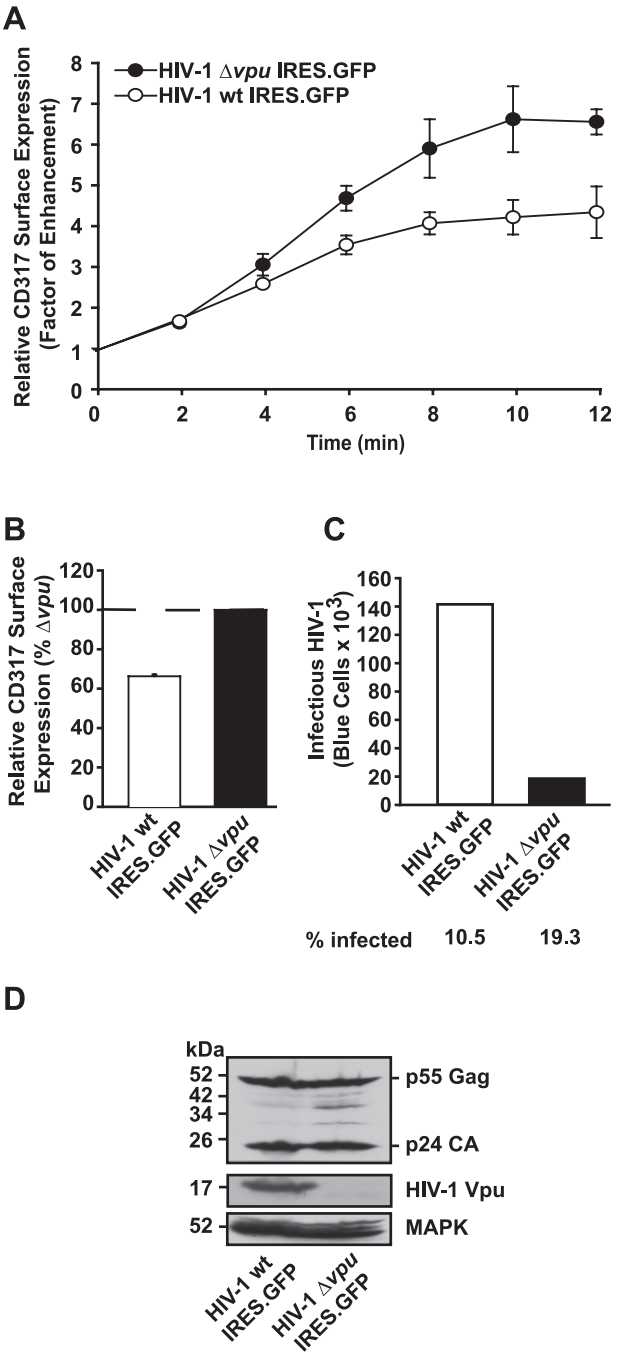

FIG 3 HIV-1-infected cells display a Vpu-dependent recycling block for CD317. TZM-bl cells were infected with either VSV-G-pseudotyped HIV-1 wt IRES.GFP or HIV-1 Δ*vpu* IRES.GFP. (A) Twenty-four hours postinfection, GFP-positive, productively infected cells were analyzed in the CD317 recycling assay. (B) Forty-eight hours postinfection, relative CD317 surface levels were analyzed on GFP-positive cells with MFI values for HIV-1 Δ*vpu* IRES.GFP-infected cells set to 100%. Shown are arithmetic means ± standard errors of the means of three independent experiments. (C) Forty-eight hours postinfection, supernatants of wt and Δ*vpu* virus-infected cultures were harvested and the release of infectious particles was assessed in a standard infectivity assay. The percentages of HIV-1-infected cells are given below the graph. (D) Corresponding cell lysates were analyzed by Western blotting for Vpu and Gag proteins. Mitogen-activated protein kinase (MAPK) served as a loading control.

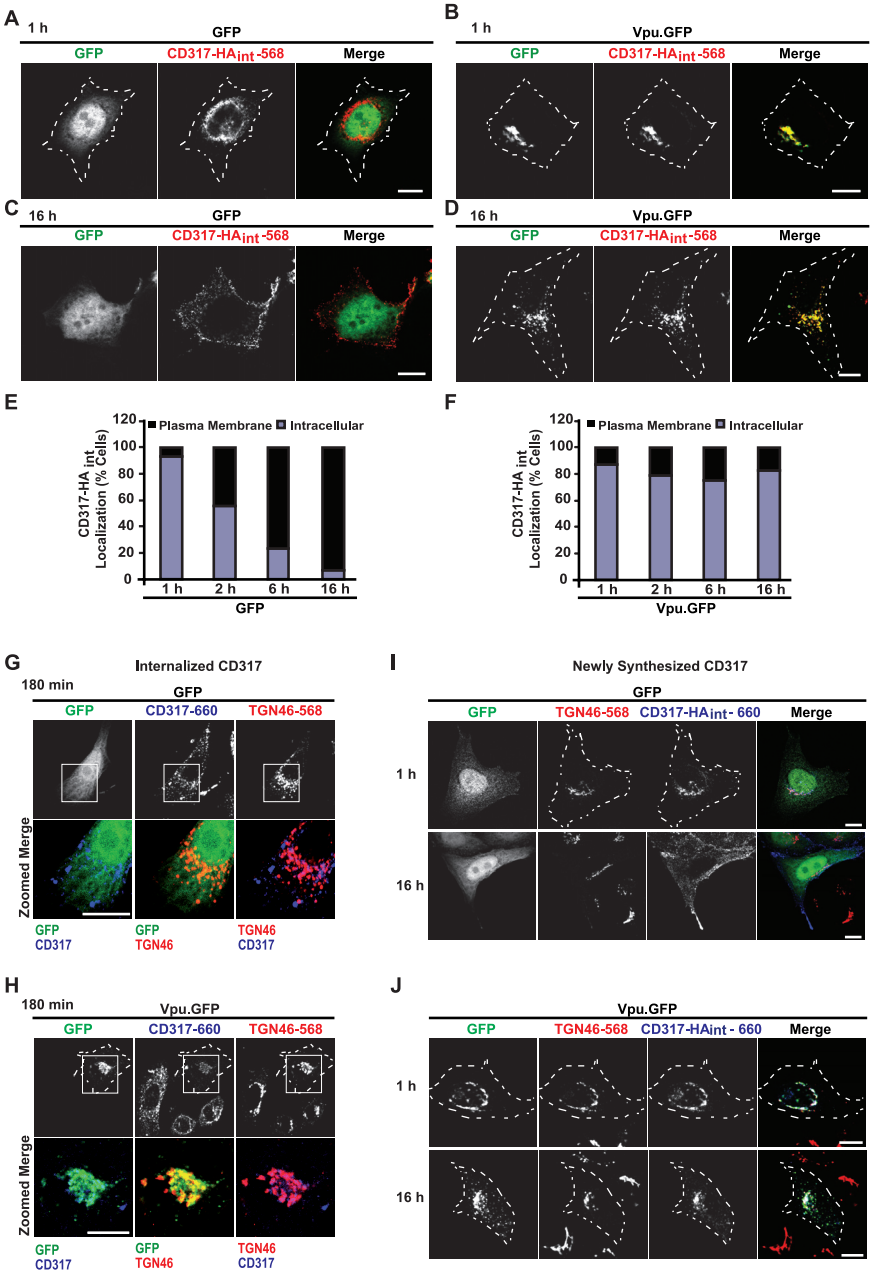

FIG 4 Vpu disrupts anterograde transport of newly synthesized CD317 to the cell surface and traps trafficking CD317 molecules in the *trans*-Golgi network. The nuclei of TZM-bl cells, grown on coverslips, were comicroinjected with a CD317-HA_{int} expression plasmid together with vectors encoding either GFP (A and C) or Vpu.GFP (B and D). Approximately 200 cells were microinjected per plasmid combination. Subsequently, cells were cultivated for 1, 2, 6, or 16 h and then fixed, permeabilized, and stained with an anti-HA MAb followed by an Alexa 568-conjugated secondary Ab (red staining) to detect newly synthesized CD317-HA_{int}. (E and F) By staining, cells were categorized as those which, besides intracellular staining, also displayed a clear plasma membrane staining ("plasma membrane") or those with an exclusive intracellular staining ("intracellular") of CD317-HA_{int} upon coexpression of either GFP (E) or Vpu.GFP (F). Histogram bars depict the relative percentage of cells for each time point from at least 150 cells that were analyzed out of three independent microinjection experiments. (G to J) Localization studies for trafficking CD317 molecules. (G and H) Internalized antibody-CD317 complexes. TZM-bl cells grown on coverslips were transfected with expression plasmids encoding either GFP or Vpu.GFP. Twenty-four hours posttransfection, cells were stained with unconjugated anti-HM1.24/CD317 MAb at 4°C before incubation at 37°C for 180 min. Anti-HM1.24 MAb–CD317 complexes were visualized in fixed and permeabilized cells using an Alexa 660-conjugated secondary antibody (blue staining). In addition, cells were stained with an anti-TGN46 Ab, which was detected with an Alexa 568-conjugated secondary antibody (red staining). Single-channel and merged confocal microphotographs for the localization of GFP or Vpu.GFP (both green), anti-HM1.24–CD317 complexes, and TGN46 are shown. (I and J) Newly synthesized CD317. TZM-bl cells were microinjected with plasmids encoding either GFP or Vpu.GFP as described above. Subsequently, cells were cultivated for 1 or 16 h and then fixed, permeabilized, and stained with an anti-HA MAb followed by an Alexa 660-conjugated secondary Ab (blue staining) and the TGN marker TGN46 (red staining). Microphotographs shown are representative for three independent experiments. In panels A, B, D, H, I, and J, cell circumferences are indicated. Scale bars, 10 μm. "Zoomed Merge" in panels G and H refers to a higher magnification of the box depicted in the image above in which the indicated color channels are superimposed.

Fig. 4D), at which not even 20% of cells displayed a detectable plasma membrane localization of CD317-HA_{int} (Fig. 4F). This striking block to CD317 surface transport was seen also for untagged Vpu coexpressed with GFP (Fig. S5A to S5C) and in HT1080 cells, which express no endogenous CD317 (9) (Fig. S5D to S5I). To test whether this defect in anterograde CD317 transport can be recapitulated in primary HIV target cells, monocyte-derived macrophages were comicroinjected with expression plasmids encoding an internally GFP-tagged CD317 (3) and plasmids for either Vpu.HcRed or the red fluorescent protein control (Fig. S6). Six hours postmicroinjection, 17 out of 21 control macrophages displayed a clear surface localization of CD317.GFP (Fig. S6A and S6C). In contrast, none of the 15 macrophages which coexpressed Vpu.HcRed had an appreciable plasma membrane expression at this time point and CD317.GFP primarily localized in a perinuclear compartment (Fig. S6B and S6C). Also 16 h postinjection, CD317 had not reached the cell surface in Vpu-positive macrophages (data not shown), indicating a severe transport defect.

To determine whether the perinuclear accumulation of CD317-HA_{int} in Vpu.GFP-expressing cells at later time points (Fig. 4D) reflected a combination of the viral proteins' impact on the trafficking of newly synthesized molecules in the anterograde pathway and that on recycling populations, a plasmid encoding the dominant negative dynamin K44A mutant fused to mCherry was comicroinjected. Coexpression of this inhibitor of CD317 en-

docytosis in TZM-bl cells (Fig. 1D) did not alter the subcellular redistribution of newly synthesized CD317-HA_{int} in Vpu.GFP-expressing cells (data not shown). This indicates that successfully plasma membrane-targeted and subsequently endocytosed molecules do not contribute significantly to the pronounced localization phenotype of CD317 in this assay. These results demonstrate the potential of Vpu to strongly inhibit the anterograde transport of newly synthesized CD317 molecules to the plasma membrane and to induce their accumulation in a perinuclear compartment.

Vpu traps trafficking CD317 molecules in the trans-Golgi network. We next performed a confocal microscopy study to characterize the long-term fate of anti-HM1.24 MAb-labeled CD317 molecules that were endocytosed from the surface of TZM-bl cells expressing either GFP or Vpu.GFP following a temperature shift from 4°C to 37°C. When we focused exclusively on the cell surface population of CD317-antibody complexes in nonpermeabilized cells, rapid removal of CD317 was observed in the presence of GFP and Vpu.GFP (Fig. S4A and S4C, compare 0 and 30 min). These internalized CD317-antibody complexes efficiently reemerged at the cell surface of GFP-expressing control cells 6 h postinternalization (Fig. S4A, left panel, and S4C), indicating that the antibody-CD317 complexes had remained intact during internalization and recycling and that full rounds of CD317 endocytosis and recycling likely take significantly longer than the resurfacing of intracellular pools that we detected by flow cytometry. Confirming our results from the FACS-based recycling assay, Vpu.GFP potently blocked this resurfacing of CD317 molecules (Fig. S4A, right panel, and Fig. S4C). Analysis of total cellular pools of CD317-antibody complexes on cells that were permeabilized prior to staining confirmed this Vpu-mediated block in CD317 recycling and indicated that Vpu retains CD317 pools that were previously internalized from the cell surface in a perinuclear compartment (Fig. S4B).

Recent reports suggested that under steady-state conditions Vpu colocalizes with CD317 in the TGN (30, 36, 54). To first test whether Vpu selectively induces an accumulation of recently endocytosed antibody-CD317 complexes in this membranous network, we conducted colocalization studies in TZM-bl cells. Indeed, Vpu.GFP expression resulted in a pronounced accumulation of anti-HM1.24 MAb-CD317 complexes in or near TGN46-positive compartments 180 min after internalization (Fig. 4H). This extensive colocalization was not observed in untransfected neighboring cells or in GFP-expressing controls (Fig. 4G). Similarly, the perinuclear compartment in which newly synthesized CD317-HA_{int} molecules accumulated in Vpu.GFP-coexpressing cells following plasmid microinjection strongly colocalized with TGN46 (Fig. 4J). Thus, both recently endocytosed and newly synthesized CD317 molecules in the anterograde transport pathway accumulate in the TGN upon Vpu coexpression. Of note, Vpu.GFP also displayed significant colocalization with this TGN-associated CD317 pool.

Inhibition of CD317 recycling and anterograde transport depends on the diserine motif in Vpu. Since the highly conserved serine residues 52 and 56 in the cytoplasmic tail of Vpu are critical for antagonizing the CD317-imposed restriction on HIV-1 particle release when expressed in *cis* or *trans* (26, 34, 55, 56), we tested whether this diserine motif affects Vpu's ability to inhibit the recycling and anterograde transport of CD317. Consistent with a number of recent reports (29, 31, 34, 55, 56), we observed that the reduction of CD317 steady-state surface levels in TZM-bl cells depended on Vpu's diserine motif, as alanine replacements of serine residues 52 and 56 (Vpu2/6) largely abrogated its downmodulating activity (Fig. 5A).

We then examined the recycling kinetics of endogenous CD317 molecules in TZM-bl cells expressing either Vpu.GFP, Vpu2/6.GFP, or GFP alone. As already shown in Fig. 2B, CD317 recycling was diminished in cells expressing Vpu.GFP compared to that in GFP-expressing control cells (Fig. 5B). Importantly, the recycling kinetic of CD317 in cells expressing the Vpu2/6.GFP mutant (Fig. 5B) or the untagged Vpu2/6 together with GFP (Fig. S7) was indistinguishable from that in corresponding GFP control cells (Fig. 5B and Fig. S7), indicating a requirement of the diserine motif for Vpu's capacity to interfere with this trafficking pathway of CD317. In addition, we also tested the involvement of the diserine motif on the block of anterograde transport of newly synthesized CD317-HA_{int} induced by the viral accessory protein. Both the kinetic and magnitude of CD317-HA_{int} anterograde transport to the cell surface in the microscopy-based *de novo* expression assay were comparable in TZM-bl cells expressing the Vpu2/6.GFP mutant (Fig. 5C, D, and E) and in cells expressing GFP alone (Fig. 4A, C, and E). Moreover, cells expressing Vpu2/6.GFP did not display the pronounced perinuclear accumulation of CD317-HA_{int} seen in the presence of Vpu.GFP (compare Fig. 5C and D and Fig. 4B and D). Together, these results suggest that serine residues 52 and 56 are essential for Vpu's inhibitory influence on both the recycling and anterograde transport of CD317 molecules.

Proteasomal degradation of CD317 and the diserine motif interactor β-TrCP are not strictly required for Vpu's ability to block CD317 recycling. The canonical diserine motif in Vpu is critical for its interaction with the substrate recognition adaptor β-TrCP, which is part of the SCF-E3 ubiquitin ligase complex. This Vpu–β-TrCP interaction is important for proteasomal and/or endolysosomal degradation of CD317 (27, 29, 31, 56). Based on the above-established importance of the diserine motif for Vpu's capacity to block intracellular CD317 trafficking, we explored the role of CD317 degradation and cellular β-TrCP levels in this process.

To study the requirement for proteasomal degradation, recycling of CD317 was first quantified in TZM-bl cells expressing GFP or Vpu.GFP in the presence of the proteasome inhibitor ALLN. Under these experimental conditions, ALLN effectively inhibited Vpu-mediated proteasomal degradation of CD4 as assessed by the fully recovered receptor's cell surface exposure (Fig. S8A). Kinetic analysis of CD317 recycling in dimethyl sulfoxide (DMSO)-treated cells confirmed the inhibition of this trafficking pathway in Vpu.GFP-expressing cells compared to GFP-expressing controls (Fig. 5F, circles). ALLN treatment lowered the basal CD317 recycling rate (Fig. 5F, compare black circles and triangles); however, Vpu.GFP was still capable of markedly reducing CD317 recycling under these conditions (Fig. 5F, triangles).

To directly assess the requirement for β-TrCP in Vpu's capacity to interfere with CD317 recycling, we employed RNA interference. TZM-bl cells were transfected twice with small interfering RNAs (siRNAs) targeting both β-TrCP isoforms, *β-TrCP1* and *β-TrCP2*. During the second transfection, expression plasmids for Vpu.GFP or GFP were added. Because antibodies for reliable detection of these β-TrCP isoforms are lacking, we recently validated the effectiveness and specificity of these siRNAs using coexpressed Myc- or Flag-tagged β-TrCP1 or β-TrCP2 constructs and estab-

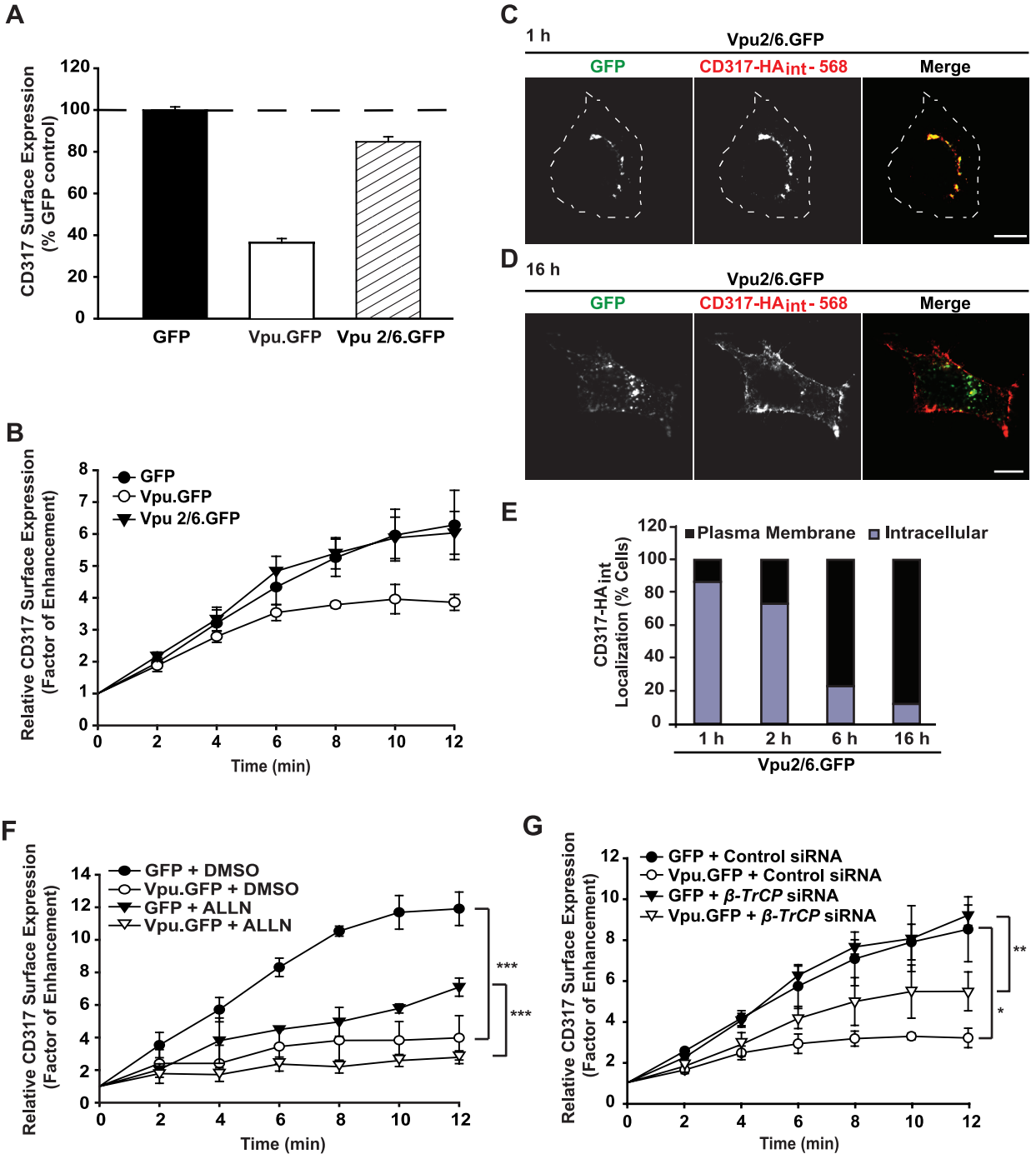

FIG 5 Vpu's ability to block CD317 recycling and anterograde transport depends on its diserine motif but not on proteasomal degradation of CD317 or β-TrCP. (A and B) Recycling CD317. TZM-bl cells were transfected with expression plasmids encoding either Vpu.GFP, Vpu2/6.GFP, or GFP. Twenty-four hours posttransfection, GFP-expressing cells were analyzed for surface steady-state levels of CD317 (A) or in the CD317 recycling assay (B). Shown are arithmetic means ± standard deviations of triplicates of one representative of three independent experiments. (C, D, and E) Newly synthesized CD317. TZM-bl cells were comicroinjected with CD317-HA_{int} and Vpu2/6.GFP expression plasmids. Cells were cultivated for 1, 2, 6, or 16 h and then fixed. Next, cells were permeabilized and stained with an Alexa 568-conjugated anti-HA MAb (red staining) to detect newly synthesized CD317-HA_{int} molecules. Microphotographs shown are representative for three independent experiments. Scale bars, 10 μm. By staining, cells were categorized as those which, besides intracellular staining, also displayed a clear plasma membrane staining ("plasma membrane") or those with an exclusive intracellular staining ("intracellular") of CD317-HA_{int} upon coexpression of Vpu2/6.GFP. For each time point, at least 150 cells out of three independent microinjection experiments were counted. (F) Inhibition of proteasomal degradation by ALLN (*N*-acetylleucylleucylnorleucinal) does not interfere with Vpu's ability to block CD317 recycling. TZM-bl cells were transfected with expression plasmids encoding either Vpu.GFP or GFP. At 6 h posttransfection, either ALLN (50 μM) or DMSO solvent was added to the culture medium for 18 h. Twenty-four hours posttransfection, Vpu.GFP/GFP-expressing cells were analyzed in the CD317 recycling assay or stained for CD4 surface expression (Fig. S4A). Shown is one representative of two independent experiments. (G) β-TrCP is not strictly required for Vpu's ability to block CD317 recycling. TZM-bl cells were transfected twice with siRNAs targeting *β-TrCP1* and *β-TrCP2* (β-TrCP siRNA) or control siRNA. At the second transfection, expression plasmids encoding either Vpu.GFP or GFP were added. Three days following the first transfection, TZM-bl cells were harvested and analyzed in the CD317 recycling assay or stained for CD317 (Fig. S4B) or CD4 (Fig. S4C) surface expression. Shown is one representative experiment of four independent experiments, and arithmetic means ± standard deviations of triplicates are depicted. Significance by Student's *t* test: *, $P < 0.05$; **, $P < 0.02$; ***, $P < 0.002$.

lished protocols for isoform-specific mRNA quantification (56). In the current study, levels of specific β-TrCP mRNAs were reduced by >90% compared to those in control siRNA-transfected cells (data not shown). As an informative Vpu–β-TrCP-dependent reference for the functionality of our gene silencing approach, Vpu.GFP completely lost its ability to degrade CD4 in *β-TrCP*-silenced cells (Fig. S8B). In contrast, Vpu.GFP still significantly downregulated CD317 surface levels in these cells (Fig. S8C), although the reduction of the surface pool was less pronounced than that in control siRNA-treated cells. Importantly and consistently, β-TrCP-depleted TZM-bl cells displayed a highly significant, albeit slightly diminished, capacity to support Vpu's inhibitory influence on CD317 recycling (Fig. 5G).

Taken together, Vpu interferes with CD317 trafficking via a mechanism that critically depends on its diserine motif, but Vpu's effect on CD317 recycling does not strictly require proteasomal degradation or the interaction with the β-TrCP substrate recognition domain of the SCF-E3 ubiquitin ligase complex in TZM-bl cells. This indicates that a yet-to-be identified cellular factor may interact with the diserine motif of Vpu to alter CD317 trafficking.

Primaquine mimics Vpu's impact on CD317 trafficking. Addition of PQ at noncytotoxic concentrations to the culture medium of TZM-bl cells for as little as 45 min down-modulated steady-state surface levels of CD317 by up to 70% (Fig. 6A) and blocked CD317 recycling (Fig. 6B and 1E). PQ, besides acting on the recycling of surface proteins (50, 51), has been suggested to inhibit the formation of functional transport vesicles involved also in the anterograde pathway of certain glycoproteins (57). We thus wondered whether PQ affects the kinetic of cell surface exposure of newly synthesized CD317 molecules. Cultivation of TZM-bl cells, which had been microinjected with the plasmid encoding CD317-HA_{int}, in the presence of PQ inhibited the appearance of CD317 at the plasma membrane (Fig. 6C and 6D), demonstrating an interference of the drug also with anterograde trafficking of CD317. While PQ affected the recycling and anterograde sorting steps that are also targeted by Vpu, the drug induced bulkier aggregated patches of CD317-HA_{int} than did Vpu.GFP (compare Fig. 6C and Fig. 4B and 4D). Interestingly, PQ had no effect on the restriction factor's endocytosis rates (Fig. S9A). Both PQ and Vpu markedly reduced surface levels of CD4 (Fig. 2A and Fig. S9B), albeit via different modes of action: PQ, in contrast to Vpu, inhibited the recycling of CD4 (compare Fig. S9C and Fig. 2D). Collectively, and similarly to Vpu, PQ potently diminishes steady-state surface levels of CD317 by interfering with both recycling and biosynthetic transport of the cellular restriction factor.

Primaquine mimics Vpu's antagonistic function. Based on the above findings, we hypothesized that Vpu's ability to interfere with both recycling and anterograde transport of CD317 could be sufficient (i) to account for the markedly reduced surface levels of the restriction factor at steady state and (ii) to overcome the CD317-imposed virion release restriction. The comparable magnitudes of CD317 downregulation by Vpu expression and that by PQ treatment at steady state and their similar patterns of interference with CD317 trafficking led us to explore whether this drug could support the release of Vpu-defective HIV-1.

To test this, TZM-bl cells were first transfected with proviral plasmids encoding either HIV-1 wt or the isogenic Vpu-defective counterpart, HIV-1 Δ*vpu* (schematic of experimental setup in Fig. 6E). Thirty-six hours later, cells were washed and PQ or solvent was added to the culture medium for 3 h. Following a second washing step to remove viruses secreted up to this point, cells were cultivated for another 3 h in the presence or absence of PQ, and virion release during this time interval was quantified by p24CA enzyme-linked immunosorbent assay (ELISA), in principle as reported previously (26, 42).

Solvent-treated TZM-bl cells (control) showed the expected Vpu-dependent virological phenotype: HIV-1 wt virions, but not HIV-1 Δ*vpu* virions, were efficiently released from transfected cells (Fig. 6F, black bars). Importantly, the release of Vpu-defective HIV-1 from PQ-treated cells was elevated ~4-fold and this release efficiency was statistically indistinguishable from that seen for HIV-1 wt (Fig. 6F). Even though PQ is known to influence different intracellular sorting processes, the release of HIV-1 wt virions was not affected by PQ treatment (Fig. 6F), excluding unspecific, Vpu-independent effects of the drug on HIV-1 production. In summary, pharmacological inhibition of CD317 trafficking by PQ resulted in a downregulation of CD317 steady-state levels that was comparable to that by Vpu in terms of magnitude and the general pattern of interference with CD317 trafficking. Most critically, this effect was sufficient to overcome the CD317-imposed release restriction for Vpu-defective HIV-1.

DISCUSSION

This study aimed at (i) identifying which step of CD317 trafficking is affected by HIV-1 Vpu to induce a reduction of steady-state cell surface levels of the restriction factor and (ii) analyzing whether this interference with CD317 trafficking may account for the counteraction of the CD317-imposed restriction on HIV-1 particle release. Using kinetic flow cytometry- and microscopy-based sorting approaches, we demonstrate that Vpu diminishes anterograde biosynthetic transport as well as recycling of CD317. In contrast, the CD317 internalization rate remained unaffected by Vpu. The block to intracellular sorting of CD317 resulted in trapping of the restriction factor at the TGN where CD317 and Vpu colocalized. The interference with CD317 transport required the highly conserved diserine motif in the cytoplasmic tail of Vpu; however, it did not depend on proteasomal degradation of CD317 or the presence of the E3 ubiquitin ligase substrate adaptor β-TrCP. Treatment of cells with the lysosomotropic amine PQ induced CD317 transport defects comparable to those observed in the presence of Vpu, and PQ could functionally replace Vpu as an antagonist for the CD317-imposed HIV-1 release restriction. Together, these results reveal that Vpu employs a dual mechanism to trap both recycling and newly synthesized pools of CD317 at intracellular membranes and establish subversion of cell surface transport as a mechanism of HIV-mediated restriction factor evasion.

As part of our comprehensive characterization of Vpu's potential effects on CD317 trafficking, we first examined receptor endocytosis. Despite downregulation of CD317 surface levels by up to 70%, the rate of CD317 internalization was not altered in the presence of HIV-1 Vpu, consistent with recent reports (30, 31, 43). These findings do not, however, exclude alterations in the route of internalization of the restriction factor from the cell surface to intracellular compartments, as recently proposed (38).

Recent reports provided the first indications that Vpu may affect intracellular trafficking of CD317 (30, 37, 40, 43, 58, 59); however, the step(s) affected as well as underlying mechanisms has remained elusive. In the current study, we employed assay

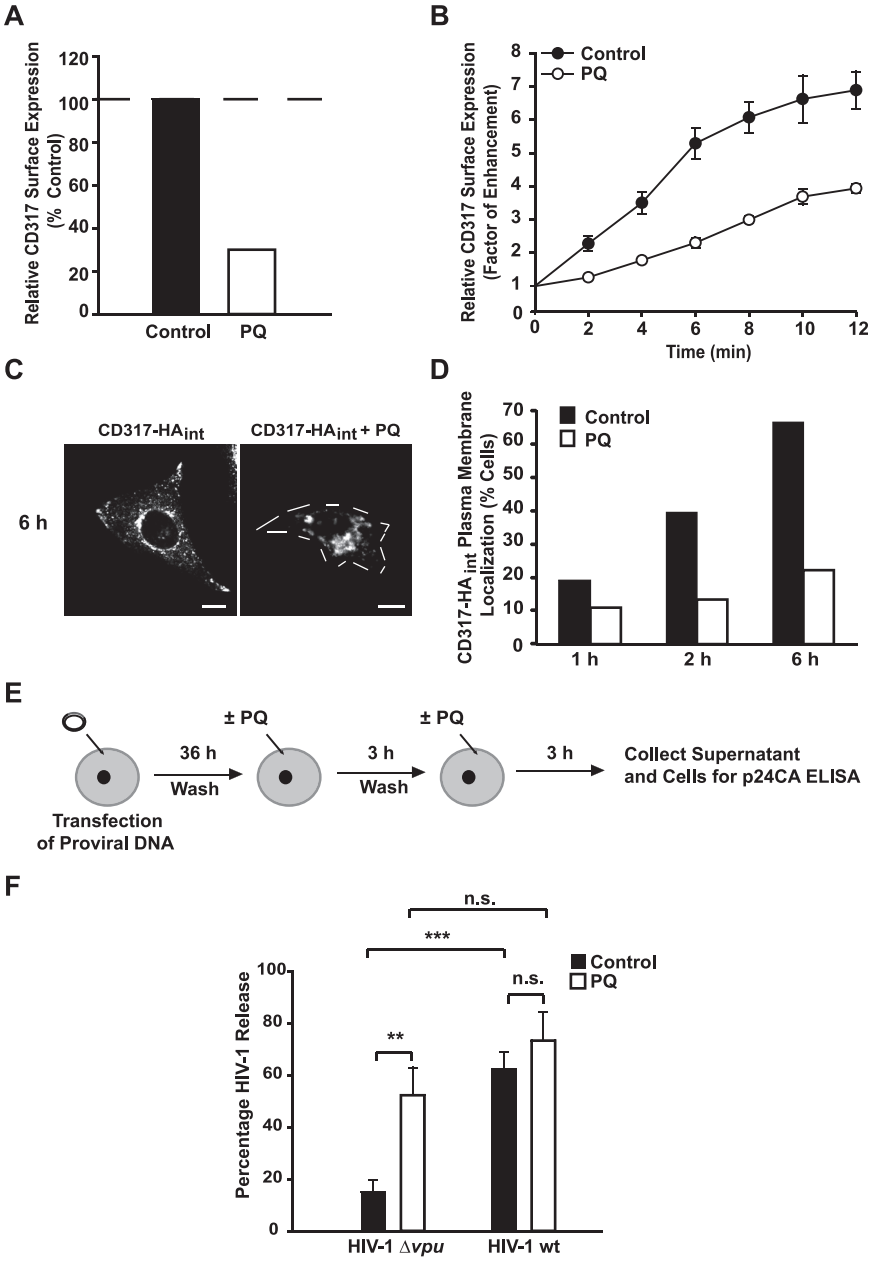

FIG 6 Primaquine, which mimics Vpu's pattern of interference with CD317 trafficking, overcomes the CD317-imposed release restriction of Vpu-defective HIV-1. (A and B) Recycling CD317. TZM-bl cells were cultivated for 45 min in the presence or absence of primaquine (PQ) (0.5 mM). Subsequently, cells were stained for surface steady-state levels of CD317 (A) and analyzed in the CD317 recycling assay as described for Fig. 1 (B). (C and D) Cells microinjected with a plasmid encoding CD317-HA_{int} and subsequently cultivated in either the presence or the absence of PQ (0.15 mM) for 6 h. Microphotographs of fixed, permeabilized, and anti-HA-stained cells shown are representative for three independent experiments. Scale bars, 10 μm. (E) Schematic representation of the HIV-1 release assay in cells cultivated in the presence or absence of PQ. TZM-bl cells were transfected with a proviral plasmid encoding either HIV-1 wt or the isogenic Vpu-defective counterpart, HIV-1 Δ*vpu*. Thirty-six hours posttransfection, cells were washed and cultivated for 3 h in either the presence or the absence of PQ (0.15 mM). Cells were washed again to remove residual virus and cultivated for an additional period of 3 h in the presence or absence of PQ. Subsequently, the p24CA concentration was quantified in concentrated culture supernatants and cell lysates using a p24CA antigen ELISA. (F) HIV-1 release was expressed as the percentage of total p24CA (in cells and supernatant) that was secreted as virion-associated p24CA, in principle as reported previously (26). Values are arithmetic means ± standard deviations of triplicates from one representative out of three independent experiments. Significance by Student's *t* test: **, $P < 0.02$; ***, $P < 0.002$; n.s., not significant.

systems that enabled us to directly determine transport kinetics of recycling as well as biosynthesized pools of CD317 on their way to the plasma membrane. We validated an antibody-based CD317 recycling assay for the kinetic and quantitative detection of molecules trafficking from intracellular pools back to the cell surface. The exclusive detection of recycling molecules in this assay is supported by (i) insensitivity to brefeldin A-induced Golgi apparatus disruption and a cycloheximide-induced block in translation; (ii) the lack of influence of Vpu on recycling of CD4 in this assay, the latter being already retained in the ER followed by targeting to the ERAD pathway (22, 24); and (iii) the exclusion of antibody shedding from presaturated CD317 surface pools. Our flow cytometric recycling assay, in contrast to previously reported approaches (45–48, 50, 60, 61), does not require potentially cytotoxic and antibody affinity-altering protease or acidic buffer treatments of cells or the induction of endocytosis by a specific ligand. In this assay, Vpu had a pronounced inhibitory effect on CD317 recycling following ectopic expression or HIV-1 infection. This principal finding was supported by results from a second, microscopy-based approach, in which a longer observation period allowed tracking of antibody-CD317 complexes that first were internalized and subsequently resurfaced. Also here, Vpu induced a block to CD317 recycling which coincided with an accumulation of endocytosed CD317 at or near the TGN.

To unambiguously assess the anterograde transport and fate of CD317 in the biosynthetic pathway, we performed kinetic microscopy-based trafficking studies on newly synthesized CD317 molecules. Nuclear microinjection of plasmid DNA allowed a rapid, strong, and synchronized *de novo* expression of both HA-tagged CD317 and Vpu.GFP. Here, Vpu drastically inhibited the transport of CD317 towards the plasma membrane. Of note, the kinetic analysis of subcellular localization of newly synthesized CD317 in Vpu-coexpressing cells provided a hint that Vpu may actually accelerate the initial transport steps of newly synthesized CD317, from the ER to the TGN, before trafficking of the restriction factor comes to a halt at the TGN. While this experimental approach cannot be transferred to HIV-1-infected cells for technical and safety reasons, this result establishes that

Vpu has the potential for interference with anterograde transport of newly synthesized CD317 molecules. In line with this finding, a previous study proposed Vpu as a regulator of trafficking along the secretory pathway (58). Together, our results provide a direct demonstration that HIV-1 Vpu interferes with recycling as well as anterograde transport of CD317 towards the plasma membrane, resulting in a net reduction of antivirally active surface levels of the restriction factor.

Notably, Vpu sequestered recycling and newly synthesized CD317 populations in a perinuclear compartment that frequently stained positive for the TGN marker TGN46 and the viral protein itself. These effects on two distinct cellular pools of trafficking CD317 molecules could in principle result from independent activities of Vpu. Based on several lines of evidence, however, we favor a direct and integrative model of Vpu's effect on CD317 trafficking. First, the Vpu-like inhibition pattern of the weak base PQ on CD317 trafficking (blocked recycling and anterograde biosynthetic transport and unaltered endocytosis) suggests the existence of common principles that govern the two intracellular transport routes. Second, the TGN represents the central sorting platform in the secretory pathway that is also in direct connection with retrograde transport pathways from early, late, and recycling endosomes (62, 63). The TGN thus likely acts as a transport checkpoint for both newly synthesized and recycling pools of CD317, rendering it an ideal compartment for intracellular trapping strategies of a viral pathogen. Finally, physical association between Vpu and CD317 via their transmembrane domains is an established requirement for antagonism of the HIV-1 release restriction (27, 30, 64–66). In light of the pronounced colocalization of Vpu with CD317 sequestered to the TGN, one can speculate that Vpu, by virtue of its constant localization at this membranous network, interacts with CD317 molecules in transit to arrest their forward transport to the cell surface irrespective of whether they are incorporated in recycling or secretory vesicles.

On a molecular level, the results presented establish a cardinal role for Vpu's diserine motif for changes induced by the viral protein to intracellular CD317 trafficking, TGN trapping of CD317, and antagonism of the HIV-1 release restriction. In the context of Vpu-mediated degradation of CD4, this motif serves as a recruitment platform for β-TrCP as part of the SCF-E3 ubiquitin ligase complex that couples the receptor to a proteasomal degradation pathway (23, 25). Importantly, Vpu still interfered with CD317 trafficking in cells, in which proteasomal degradation was inhibited or β-TrCP was silenced. Moreover, we could recently show that both degradation of CD317 (33) and β-TrCP expression (56) are not strictly required for Vpu antagonism. Collectively, these findings argue for a decisive role of the diserine motif in Vpu during TGN trapping of CD317 that is different from its β-TrCP-dependent function exerted in the context of targeted CD4 degradation. The diserine motif in Vpu's cytoplasmic tail represents a bona fide protein interaction site in its phosphorylated form that is, however, not involved in the transmembrane domain-dependent association of Vpu and CD317 (27, 30, 64–66). Since phosphorylation of these serine residues is apparently required for functional antagonism of CD317 by Vpu (55), we hypothesize that the cardinal role of the Vpu diserine motif reflects the interaction with a yet-to-be-identified host cell protein(s) distinct from β-TrCP. In this scenario, the frequently observed Vpu-mediated degradation of CD317 via proteasomal and/or lysosomal pathways reported by us and many other laboratories (26–29, 32, 33, 67) would likely be a secondary consequence of altered sorting or mistrafficking of the restriction factor. While CD317 degradation clearly occurs in relevant cell systems, including infected CD4 T cells (26), it does not appear to be strictly required for Vpu's function as a CD317 antagonist.

The identification of a Vpu-like phenotype imprinted on CD317 trafficking by PQ allowed us to independently address the functional consequence of this dual trafficking block on CD317 steady-state surface levels and on the release of Vpu-defective HIV-1. Remarkably, PQ was a functional phenocopy of Vpu in promoting virus release in cells expressing high levels of endogenous CD317. While PQ and Vpu are likely to affect recycling and anterograde transport of CD317 via distinct molecular mechanisms, these results demonstrate that inhibition of select CD317 plasma membrane transport pathways is sufficient to markedly reduce CD317 surface levels. Furthermore, this suggests trafficking interference as a central mechanism employed by Vpu to overcome the particle release restriction.

Consistent with the correlation between the reduction of CD317 surface exposure and enhancement of HIV-1 release induced by Vpu (29, 31, 33, 34), this supports the model that surface density of CD317 is critical for physical tethering of virions at the plasma membrane of virus-producing cells. It is noteworthy that the (at most) 4-fold reduction of CD317 steady-state cell surface levels induced by Vpu is not proportional in magnitude to its ability to promote virion release (10- to 1,000-fold enhancement). Similarly, the potent interference of Vpu with CD317 plasma membrane transport kinetics could be expected to cause a more severe drop in steady-state surface levels of the restriction factor. This might suggest the existence of CD317 subpopulations with distinct trafficking characteristics and/or susceptibility to Vpu. In this scenario, recycling as well as secretory pools of CD317 may conceivably have a higher antiviral potential than molecules that reside at the cell surface for extended periods of time and are not subject to frequent internalization. This model could reconcile Vpu's pronounced ability to enhance virus release while only moderately reducing overall cell surface levels of the restriction factor. Vpu-mediated antagonism of CD317 may thus induce quantitative as well as qualitative alterations of cell surface pools of the restriction factor. Together, our findings establish disruption of specific intracellular transport pathways of an antiviral host factor as an immune escape mechanism employed by HIV-1.

MATERIALS AND METHODS

Plasmids. The plasmid pcDNA-Vphu, expressing a codon-optimized, Rev-independent HIV-1_{NL4-3} Vpu protein, was from Klaus Strebel. Vphu S52AS56A (Vpu2/6A) was generated by site-directed mutagenesis from pcDNA-Vphu (26). Constructs encoding codon-optimized Vpu and VpuS52/56A fused to enhanced GFP (eGFP) (Vpu.GFP and Vpu2/6A.GFP) have been reported previously (54). The plasmid encoding human CD317, which carries the HA tag sequence inserted immediately 3′ of *CD317* codon 154 (referred to as CD317-HA_{int}) was provided by Paul D. Bieniasz (35). Constructs encoding dominant negative dynamin fused to either GFP (dynamin K44A.GFP) or mCherry (DynK44A.mCherry) were provided by Ari Helenius and Hans-Georg Kräusslich, respectively. Plasmids for CD317-GFP_{int} (3) and Vpu.HcRed (59) were from George Banting and Paul Spearman, respectively.

CD317 and CD4 recycling assay. Recycling assays for CD317 and CD4 were performed in principle as depicted in Fig. 1A. TZM-bl cells were transfected with constructs encoding Vpu.GFP, Vpu2/6.GFP, or GFP or were infected with VSV-G-pseudotyped HIV-1_{NL4-3} wt IRES.GFP or

HIV-1_{NL4-3} Δ*vpu* IRES.GFP. Twenty-four hours posttransfection or postinfection, cells were first incubated with saturating concentrations of the unconjugated anti-HM1.24 MAb or anti-CD4 MAb (clone RPA-T4; BD Pharmingen) in ice-cold binding medium (Dulbecco's modified Eagle's medium supplemented with 2% fetal bovine serum and 20 mM HEPES, pH 7.5) at 4°C. Cells were then washed in binding medium before being shifted to 37°C for 0 to 12 min. Subsequently, cells were placed on ice followed by incubation with either APC-conjugated anti-HM1.24 MAb or APC-conjugated anti-CD4 MAb (clone RPA-T4). For coupling of anti-HM1.24 MAb, the APC fluorophore Lightning Link kit (Innova Biosciences) was used according to the manufacturer's protocol. Recycling of receptors was quantified by flow cytometry analyzing the APC MFI, which reflects receptor molecules newly exposed on the surface of viable cells with identical GFP intensities (red gate indicated in Fig. 1B) during the kinetic. The APC MFIs at different time points are presented as factors of enhancement relative to the MFI at $t = 0$, which was set to 1.

CD317 anterograde biosynthetic transport assay. TZM-bl or HT1080 cells or primary human macrophages, which were grown on coverslips, were microinjected in their nuclei with an AIS 2 microinjection apparatus using pulled borosilicate glass capillaries in principle as reported previously (68). Plasmids encoding CD317-HA_{int} or CD317.GFP and either GFP, Vpu.GFP, Vpu2/6.GFP, or Vpu.HcRed were mixed in water at concentrations of 7 ng/μl and 10 ng/μl, respectively, and coinjected. Following microinjection, cells were cultured for 1, 2, 6, or 16 h at 37°C to allow protein expression and trafficking. At the indicated time points, cells were fixed with 4% paraformaldehyde–phosphate-buffered saline (PBS) and CD317-HA_{int} molecules were detected using a mouse anti-HA MAb (Santa Cruz) followed by a goat anti-mouse Alexa 568 secondary antibody (Invitrogen). Stained cells were imaged with a Zeiss LSM 510 confocal microscope.

ACKNOWLEDGMENTS

We thank Hans-Georg Kräusslich for support and reagents. We are grateful to George Banting, Paul Bieniasz, Valerie Bosch, Ari Helenius, Frank Kirchhoff, Paul Spearman, Klaus Strebel, and Chugai Pharmaceuticals for the gift of reagents. We thank Nico Michel for contributions to the design of the recycling assay, members of the Fackler and Keppler laboratories for comments on the manuscript, and SFB638 for access to the LSM510 confocal microscope.

This work was in part funded by the Deutsche Forschungsgemeinschaft (KE742/4-1) (to O.T.K. and O.T.F.). O.T.F. and O.T.K. are members of the CellNetworks Cluster of Excellence EXC81.

SUPPLEMENTAL MATERIAL

Supplemental material for this article may be found at http://mbio.asm.org/lookup/suppl/doi:10.1128/mBio.00036-11/-/DCSupplemental.

Text S1, DOC file, 0.059 MB.
Figure S1, EPS file, 1.066 MB.
Figure S2, EPS file, 2.877 MB.
Figure S3, EPS file, 0.760 MB.
Figure S4, TIF file, 1.905 MB.
Figure S5, TIF file, 1.112 MB.
Figure S6, TIF file, 0.598 MB.
Figure S7, EPS file, 0.584 MB.
Figure S8, EPS file, 0.954 MB.
Figure S9, EPS file, 0.838 MB.

REFERENCES

1. **Song B.** 2009. TRIM5alpha. Curr. Top. Microbiol. Immunol. **339**:47–66.
2. **Malim MH, Emerman M.** 2008. HIV-1 accessory proteins—ensuring viral survival in a hostile environment. Cell Host Microbe **3**:388–398.
3. **Kupzig S, et al.** 2003. Bst-2/HM1.24 is a raft-associated apical membrane protein with an unusual topology. Traffic **4**:694–709.
4. **Swiecki M, et al.** 2011. Structural and biophysical analysis of BST-2/tetherin ectodomains reveals an evolutionary conserved design to inhibit virus release. J. Biol. Chem. **286**:2987–2997.
5. **Schubert HL, et al.** 2010. Structural and functional studies on the extracellular domain of BST2/tetherin in reduced and oxidized conformations. Proc. Natl. Acad. Sci. U. S. A. **107**:17951–17956.
6. **Yang H, et al.** 2010. Structural insight into the mechanisms of enveloped virus tethering by tetherin. Proc. Natl. Acad. Sci. U. S. A. **107**:18428–18432.
7. **Rollason R, Korolchuk V, Hamilton C, Schu P, Banting G.** 2007. Clathrin-mediated endocytosis of a lipid-raft-associated protein is mediated through a dual tyrosine motif. J. Cell Sci. **120**:3850–3858.
8. **Masuyama N, et al.** 2009. HM1.24 is internalized from lipid rafts by clathrin-mediated endocytosis through interaction with alpha-adaptin. J. Biol. Chem. **284**:15927–15941.
9. **Neil SJ, Zang T, Bieniasz PD.** 2008. Tetherin inhibits retrovirus release and is antagonized by HIV-1 Vpu. Nature **451**:425–430.
10. **Hinz A, et al.** 2010. Structural basis of HIV-1 tethering to membranes by the BST-2/tetherin ectodomain. Cell Host Microbe **7**:314–323.
11. **Casartelli N, et al.** 2010. Tetherin restricts productive HIV-1 cell-to-cell transmission. PLoS Pathog. **6**:e1000955.
12. **Kuhl BD, et al.** 2010. Tetherin restricts direct cell-to-cell infection of HIV-1. Retrovirology **7**:115.
13. **Jolly C, Booth NJ, Neil SJ.** 2010. Cell-cell spread of human immunodeficiency virus type 1 overcomes tetherin/BST-2-mediated restriction in T cells. J. Virol. **84**:12185–12199.
14. **Jouvenet N, et al.** 2009. Broad-spectrum inhibition of retroviral and filoviral particle release by tetherin. J. Virol. **83**:1837–1844.
15. **Sakuma T, Noda T, Urata S, Kawaoka Y, Yasuda J.** 2009. Inhibition of Lassa and Marburg virus production by tetherin. J. Virol. **83**:2382–2385.
16. **Kaletsky RL, Francica JR, Agrawal-Gamse C, Bates P.** 2009. Tetherin-mediated restriction of filovirus budding is antagonized by the *Ebola* glycoprotein. Proc. Natl. Acad. Sci. U. S. A. **106**:2886–2891.
17. **Mansouri M, et al.** 2009. Molecular mechanism of BST2/tetherin downregulation by K5/MIR2 of Kaposi's sarcoma-associated herpesvirus. J. Virol. **83**:9672–9681.
18. **Pardieu C, et al.** 2010. The RING-CH ligase K5 antagonizes restriction of KSHV and HIV-1 particle release by mediating ubiquitin-dependent endosomal degradation of tetherin. PLoS Pathog. **6**:e1000843.
19. **Radoshitzky SR, et al.** 2010. Infectious Lassa virus, but not filoviruses, is restricted by BST-2/tetherin. J. Virol. **84**:10569–10580.
20. **Weidner JM, et al.** 2010. Interferon-induced cell membrane proteins, IFITM3 and tetherin, inhibit vesicular stomatitis virus infection via distinct mechanisms. J. Virol. **84**:12646–12657.
21. **Willey RL, Maldarelli F, Martin MA, Strebel K.** 1992. Human immunodeficiency virus type 1 Vpu protein regulates the formation of intracellular gp160-CD4 complexes. J. Virol. **66**:226–234.
22. **Magadán JG, et al.** 2010. Multilayered mechanism of CD4 downregulation by HIV-1 Vpu involving distinct ER retention and ERAD targeting steps. PLoS Pathog. **6**:e1000869.
23. **Margottin F, et al.** 1998. A novel human WD protein, h-beta TrCp, that interacts with HIV-1 Vpu connects CD4 to the ER degradation pathway through an F-box motif. Mol. Cell **1**:565–574.
24. **Binette J, et al.** 2007. Requirements for the selective degradation of CD4 receptor molecules by the human immunodeficiency virus type 1 Vpu protein in the endoplasmic reticulum. Retrovirology **4**:75.
25. **Butticaz C, Michielin O, Wyniger J, Telenti A, Rothenberger S.** 2007. Silencing of both beta-TrCP1 and HOS (beta-TrCP2) is required to suppress human immunodeficiency virus type 1 Vpu-mediated CD4 downmodulation. J. Virol. **81**:1502–1505.
26. **Goffinet C, et al.** 2009. HIV-1 antagonism of CD317 is species specific and involves Vpu-mediated proteasomal degradation of the restriction factor. Cell Host Microbe **5**:285–297.
27. **Mangeat B, et al.** 2009. HIV-1 Vpu neutralizes the antiviral factor tetherin/BST-2 by binding it and directing its beta-TrCP2-dependent degradation. PLoS Pathog. **5**:e1000574.
28. **Bartee E, McCormack A, Früh K.** 2006. Quantitative membrane proteomics reveals new cellular targets of viral immune modulators. PLoS Pathog. **2**:e107.
29. **Douglas JL, et al.** 2009. Vpu directs the degradation of the human immunodeficiency virus restriction factor BST-2/tetherin via a {beta}-TrCP-dependent mechanism. J. Virol. **83**:7931–7947.
30. **Dubé M, et al.** 2010. Antagonism of tetherin restriction of HIV-1 release by Vpu involves binding and sequestration of the restriction factor in a perinuclear compartment. PLoS Pathog. **6**:e1000856.
31. **Mitchell RS, et al.** 2009. Vpu antagonizes BST-2-mediated restriction of

HIV-1 release via beta-TrCP and endo-lysosomal trafficking. PLoS Pathog. **5**:e1000450.
32. **Miyagi E, Andrew AJ, Kao S, Strebel K.** 2009. Vpu enhances HIV-1 virus release in the absence of Bst-2 cell surface down-modulation and intracellular depletion. Proc. Natl. Acad. Sci. U. S. A. **106**:2868–2873.
33. **Goffinet C, et al.** 2010. Antagonism of CD317 restriction of human immunodeficiency virus type 1 (HIV-1) particle release and depletion of CD317 are separable activities of HIV-1 Vpu. J. Virol. **84**:4089–4094.
34. **Van Damme N, et al.** 2008. The interferon-induced protein BST-2 restricts HIV-1 release and is downregulated from the cell surface by the viral Vpu protein. Cell Host Microbe **3**:245–252.
35. **Perez-Caballero D, et al.** 2009. Tetherin inhibits HIV-1 release by directly tethering virions to cells. Cell **139**:499–511.
36. **Dubé M, et al.** 2009. Suppression of tetherin-restricting activity upon human immunodeficiency virus type 1 particle release correlates with localization of Vpu in the trans-Golgi network. J. Virol. **83**:4574–4590.
37. **Hauser H, et al.** 2010. HIV-1 Vpu and HIV-2 Env counteract BST-2/tetherin by sequestration in a perinuclear compartment. Retrovirology **7**:51.
38. **Iwabu Y, et al.** 2009. HIV-1 accessory protein Vpu internalizes cell-surface BST-2/tetherin through transmembrane interactions leading to lysosomes. J. Biol. Chem. **284**:35060–35072.
39. **Iwabu Y, Fujita H, Tanaka Y, Sata T, Tokunaga K.** 2010. Direct internalization of cell-surface BST-2/tetherin by the HIV-1 accessory protein Vpu. Commun. Integr. Biol. **3**:366–369.
40. **Dubé M, Bego MG, Paquay C, Cohen ÉA.** 2010. Modulation of HIV-1-host interaction: role of the Vpu accessory protein. Retrovirology **7**:114.
41. **Kuhl BD, Cheng V, Wainberg MA, Liang C.** 2011. Tetherin and its viral antagonists. J. Neuroimmune Pharmacol. **6**:188–201.
42. **Goffinet C, Schmidt S, Kern C, Oberbremer L, Keppler OT.** 2010. Endogenous CD317/tetherin limits replication of HIV-1 and murine leukemia virus in rodent cells and is resistant to antagonists from primate viruses. J. Virol. **84**:11374–11384.
43. **Andrew AJ, Miyagi E, Strebel K.** 2011. Differential effects of human immunodeficiency virus type 1 Vpu on the stability of BST-2/tetherin. J. Virol. **85**:2611–2619.
44. **Ohtomo T, et al.** 1999. Molecular cloning and characterization of a surface antigen preferentially overexpressed on multiple myeloma cells. Biochem. Biophys. Res. Commun. **258**:583–591.
45. **Keller GA, Siegel MW, Caras IW.** 1992. Endocytosis of glycophospholipid-anchored and transmembrane forms of CD4 by different endocytic pathways. EMBO J. **11**:863–874.
46. **Nagy G, et al.** 2006. Regulation of CD4 expression via recycling by HRES-1/RAB4 controls susceptibility to HIV infection. J. Biol. Chem. **281**:34574–34591.
47. **Signoret N, Pelchen-Matthews A, Mack M, Proudfoot AE, Marsh M.** 2000. Endocytosis and recycling of the HIV coreceptor CCR5. J. Cell Biol. **151**:1281–1294.
48. **Kershaw T, Wavre-Shapton ST, Signoret N, Marsh M.** 2009. Analysis of chemokine receptor endocytosis and intracellular trafficking. Methods Enzymol. **460**:357–377.
49. **Ochoa GC, et al.** 2000. A functional link between dynamin and the actin cytoskeleton at podosomes. J. Cell Biol. **150**:377–389.
50. **Reid PA, Watts C.** 1990. Cycling of cell-surface MHC glycoproteins through primaquine-sensitive intracellular compartments. Nature **346**:655–657.
51. **van Weert AW, Geuze HJ, Groothuis B, Stoorvogel W.** 2000. Primaquine interferes with membrane recycling from endosomes to the plasma membrane through a direct interaction with endosomes which does not involve neutralisation of endosomal pH nor osmotic swelling of endosomes. Eur. J. Cell Biol. **79**:394–399.
52. **Woods AJ, White DP, Caswell PT, Norman JC.** 2004. PKD1/PKCmu promotes alphavbeta3 integrin recycling and delivery to nascent focal adhesions. EMBO J. **23**:2531–2543.
53. **Wildum S, Schindler M, Münch J, Kirchhoff F.** 2006. Contribution of Vpu, Env, and Nef to CD4 down-modulation and resistance of human immunodeficiency virus type 1-infected T cells to superinfection. J. Virol. **80**:8047–8059.
54. **Habermann A, et al.** 2010. CD317/tetherin is enriched in the HIV-1 envelope and downregulated from the plasma membrane upon virus infection. J. Virol. **84**:4646–4658.
55. **Schindler M, et al.** 2010. Vpu serine 52 dependent counteraction of tetherin is required for HIV-1 replication in macrophages, but not in ex vivo human lymphoid tissue. Retrovirology **7**:1.
56. **Tervo HM, et al.** 2011. beta-TrCP is dispensable for Vpu's ability to overcome the CD317/tetherin-imposed restriction to HIV-1 release. Retrovirology **8**:9.
57. **Hiebsch RR, Raub TJ, Wattenberg BW.** 1991. Primaquine blocks transport by inhibiting the formation of functional transport vesicles. Studies in a cell-free assay of protein transport through the Golgi apparatus. J. Biol. Chem. **266**:20323–20328.
58. **Vincent MJ, Abdul Jabbar M.** 1995. The human immunodeficiency virus type 1 Vpu protein: a potential regulator of proteolysis and protein transport in the mammalian secretory pathway. Virology **213**:639–649.
59. **Varthakavi V, et al.** 2006. The pericentriolar recycling endosome plays a key role in Vpu-mediated enhancement of HIV-1 particle release. Traffic **7**:298–307.
60. **Blagoveshchenskaya AD, Thomas L, Feliciangeli SF, Hung CH, Thomas G.** 2002. HIV-1 Nef downregulates MHC-I by a PACS-1- and PI3K-regulated ARF6 endocytic pathway. Cell **111**:853–866.
61. **Naughtin MJ, et al.** 2010. The myotubularin phosphatase MTMR4 regulates sorting from early endosomes. J. Cell Sci. **123**:3071–3083.
62. **Johannes L, Popoff V.** 2008. Tracing the retrograde route in protein trafficking. Cell **135**:1175–1187.
63. **Pfeffer SR.** 2009. Multiple routes of protein transport from endosomes to the trans Golgi network. FEBS Lett. **583**:3811–3816.
64. **Vigan R, Neil SJ.** 2010. Determinants of tetherin antagonism in the transmembrane domain of the human immunodeficiency virus type 1 Vpu protein. J. Virol. **84**:12958–12970.
65. **Kobayashi T, et al.** 2011. Identification of amino acids in the human tetherin transmembrane domain responsible for HIV-1 Vpu interaction and susceptibility. J. Virol. **85**:932–945.
66. **Rong L, et al.** 2009. The transmembrane domain of BST-2 determines its sensitivity to down-modulation by human immunodeficiency virus type 1 Vpu. J. Virol. **83**:7536–7546.
67. **Gupta RK, et al.** 2009. Mutation of a single residue renders human tetherin resistant to HIV-1 Vpu-mediated depletion. PLoS Pathog. **5**:e1000443.
68. **Fackler OT, Luo W, Geyer M, Alberts AS, Peterlin BM.** 1999. Activation of Vav by Nef induces cytoskeletal rearrangements and downstream effector functions. Mol. Cell **3**:729–739.